

Spherical confinement of Coulombic systems inside an impenetrable box: H atom and the Hulthén potential

Amlan K. Roy*

Division of Chemical Sciences,

Indian Institute of Science Education and Research Kolkata,

Mohanpur Campus, Nadia, 741252, India

Abstract

The generalized pseudospectral method is employed to study spherical confinement in two simple Coulombic systems: (i) well celebrated and heavily studied H atom (ii) relatively less explored Hulthén potential. In both instances, *arbitrary* cavity size, as well as *low and higher states* are considered. Apart from bound state eigenvalues, eigenfunctions, expectation values, quite accurate estimates of the critical cage radius for H atom for all the 55 states corresponding to $n \leq 10$, are also examined. Some of the latter are better than previously reported values. Degeneracy and energy ordering under the isotropic confinement situation are discussed as well. The method produces consistently high-quality results for both potentials for *small as well as large* cavity size. For the H atom, present results are comparable to best theoretical values, while for the latter, this work gives considerably better estimates than all existing work so far.

Keywords: Spherical confinement, H-atom, Hulthén potential, impenetrable wall, generalized pseudospectral method, critical cage radius, screened Coulomb potential.

*Email: akroy@iiserkol.ac.in, akroy6k@gmail.com, Ph: +91-3473-279137, Fax: +91-33-25873020.

I. INTRODUCTION

Enclosure of an atom/molecule in a spherically impenetrable box was first conceived as early as in 1937 [1], where the effects of high pressure on energy levels, polarizability and ionization potential were studied. A many-electron system trapped inside an inert cavity with such a boundary experiences spatial confinement that affects its physical and chemical properties. This has, therefore, been employed in a variety of situations, e.g., the cell-model of liquid state, high-pressure physics, study of impurities in semiconductor materials, matrix isolated molecules, endohedral complexes of fullerenes, zeolites cages, helium droplets, nano-bubbles, etc. [2–8]. This has also found astrophysical applications, such as hydrogen atom spectra [9], mass-radius relation in theory of white dwarfs, determination of rate of escape of stars from galactic and globular clusters, simulation of the interiors of giant planets Jupiter and Saturn [10], etc. The recent upsurge of interest in nanotechnology has also inspired extensive research activity to simulate spatially confined quantum systems (on a scale comparable to their de Broglie wave length). Importance of such *artificial* atoms has been realized in quantum wells, quantum wires, quantum dots as well as nano-sized circuits such as quantum computer, etc., by employing a wide variety of confining potentials.

Ever since the pioneering model of [1] on compressed quantum systems, an enormous amount of work has been reported on confined hydrogen atom (CHA) problem, in particular. Effect of isotropic compression on $1s$, $2s$ and $2p$ levels of H atom were provided through a semi-quantitative calculation [11]. These [1, 11] and other following work [12] invoked a direct solution of relevant Schrödinger equation imposing the boundary condition that wave function vanishes at the surface of enclosing sphere. A Hartree-Fock self-consistent field solution [13] with Slater-type orbitals and cut-off functions has been proposed. Approximate analytical formulas for CHA eigenvalues were derived using Vawter's $\coth z$ method [14], joint perturbation method and Padé approximation [15, 16], WKB method [17]. Some other attempts are: a combined hyper-virial theorem and perturbation theory [18], a variational boundary perturbation method with appropriate cut-off function [19, 20] along with its variants [21, 22], by extending a power-series solution [23], originally proposed for free quantum systems, to confined case [24], self-consistent solution [25] of relevant Kohn-Sham equation within the broad domain of density functional theory, variational perturbation theory [26], variational method in conjunction with super-symmetric quantum mechanics [27, 28],

Rayleigh-Schrödinger perturbation theory [29], Lie algebraic treatment [29], Lagrange-mesh method [30], searching the zeros of hyper-geometric function [31], asymptotic iteration method [32], etc. So far the most accurate calculations are those based on formal solution of confluent hyper-geometric function and series method [33]. Exact solutions for this system are expressed directly in terms of Kummer M -function (confluent hyper-geometric) [34]. Some numerical schemes have also been proposed, e.g., [35]. While the dependence of ground- and excited-state energies on cage radius remained in the center of investigation in all these mentioned works, a host of other properties have all also found attention. A few notable ones are: hyperfine splitting constant [13, 16, 24, 33, 36], dipole shielding factor [37], nuclear magnetic screening constant [24, 33, 36], pressure [16, 24, 33, 36], excited-state life time [35], nuclear volume isotope effect [35], density derivatives at the nucleus [38] etc. A significant amount of work exists on static and dynamic polarizability [24, 33, 36, 37, 39–46] within the Kirkwood, Buckingham, Unsold approximations and many other methods as well. It offers some interesting properties in higher dimensions [31] as well. Confinement within *penetrable* boundaries [36, 47, 48] are studied. Shannon and Fisher information entropies in position and momentum space of CHA in soft as well as hard spherical cavities have been investigated [49, 50]. Various scaling relations are proposed [51]. Another interesting aspect of this problem is that as the confining radius decreases, binding energy decreases and there exists a *critical* value of this radius (r_c), at which latter becomes zero. Many attempts have been made to estimate this [52]. Numerous other features of CHA as well as the methods employed could be found in the elegant reviews [53–55] and references therein.

This work is concerned with the spherical confinement inside an impenetrable cavity of two widely used Coulombic systems, *viz.*, H atom and Hulthén potential. For this, the generalized pseudospectral (GPS) method is invoked, which has been found to be quite successful for a number of problems [56–63]. However, its application to confinement situations has rather been limited: H atom and Davidson oscillator [61], 3D polynomial oscillator including the harmonic oscillator [63]. Although a detailed study was made in the latter case, for H atom, only a few s and p states (a total of 9) were reported. Given the success of this approach for bound states of a variety of problems (as given in the references and therein), it is desirable to assess and validate its performance for other relevant confinement studies. With this in mind, here we thus present its extension in the context of confined H atom case in terms of eigenvalues, eigenfunctions, radial densities and various

expectation values. Besides, the critical box radius, r_c^c , for all the 55 states in H atom, are given. Small, medium and large box sizes have been used. Energy variations with respect to the cage radius, r_c , are followed for *low and high* excited states. Moreover, while a vast amount of work is published for confinement in H atom, much lesser attempts are known to understand its effects on other Coulombic systems. To follow this, the case of Hulthén potential is considered, which represents an important short-range potential. Applications are found in particle physics, atomic physics, solid-state physics and chemical physics (see, for example, the references [64–68] and therein). Over the years, numerous methods have been proposed for accurate estimation of its bound states in the *free* system. Some scattered works have been published for this potential under spherical confinement as well [17, 28]. We offer accurate bound-state energies of confined Hulthén potential for ground and some low-lying states for varying range of screening parameter. Small as well as large r_c has been considered in a systematic manner. The article is organized as follows: Section II gives a brief outline of our method, a discussion of the results are presented in Section III, while some concluding remarks are offered in Section IV.

II. THE GPS METHOD FOR CONFINEMENT

Various features of the methodology were discussed detail in previous references [56–63]. Here, only the essential details, necessary for solution of relevant single-particle Schrödinger equation for a central potential under the influence of a spherical confinement, are presented. One seeks the solution of following time-independent non-relativistic eigenvalue equation:

$$\left[-\frac{1}{2} \frac{d^2}{dr^2} + \frac{\ell(\ell+1)}{2r^2} + v(r) \right] \psi_{n,\ell}(r) = E_{n,\ell} \psi_{n,\ell}(r), \quad (1)$$

where $v(r)$ characterizes the specific potential under investigation, whereas n, ℓ refer to the usual radial and angular quantum numbers. Our interest lies in the following two cases,

$$v(r) = \begin{cases} -\frac{1}{r}, & \text{for H atom} \\ -\frac{\delta e^{-\delta r}}{1-e^{-\delta r}}, & \text{for Hulthén potential,} \end{cases} \quad (2)$$

where δ is a screening parameter. The spherical confinement is achieved by introducing the following potential as $v_c(r) = +\infty$ for $r > r_c$ and 0 for $r \leq r_c$, where r_c signifies the radius of spherical enclosure. One needs to solve this equation satisfying the Dirichlet boundary condition, $\psi_{n,\ell}(0) = \psi_{n,\ell}(r_c) = 0$.

The crucial step is to approximate a function $f(x)$ defined in the interval $x \in [-1, 1]$ by an N -th order polynomial $f_N(x)$,

$$f(x) \cong f_N(x) = \sum_{j=0}^N f(x_j) g_j(x), \quad (3)$$

so that the approximation is *exact* at *collocation points* x_j , i.e., $f_N(x_j) = f(x_j)$. Here the Legendre pseudospectral method is employed, with $x_0 = -1$, $x_N = 1$; while $x_j (j = 1, \dots, N-1)$ are to be obtained from roots of first derivative of Legendre polynomial $P_N(x)$ with respect to x ($P'_N(x_j) = 0$). The $g_j(x)$ in Eq. (3) are called cardinal functions satisfying the relation, $g_j(x_{j'}) = \delta_{j'j}$. At this stage, the semi-infinite domain $r \in [0, \infty]$ is mapped onto the finite domain $x \in [-1, 1]$ through a transformation $r = r(x)$. Next, a nonlinear algebraic mapping of the following form is introduced, for convenience,

$$r = r(x) = L \frac{1+x}{1-x+\alpha}, \quad (4)$$

where L and $\alpha = 2L/r_{max}$ are two adjustable mapping parameters. Then, introduction of a transformation of the type $\psi(r(x)) = \sqrt{r'(x)}f(x)$, followed by a symmetrization procedure leads to a *symmetric* matrix eigenvalue problem. This is easily solved by standard available routines (NAG libraries, for example) offering quite accurate eigenvalues and eigenfunctions.

III. RESULTS AND DISCUSSION

A. Confined H atom

At first, Table I gives energies of H atom at the center of an inert impenetrable cavity for two lowest-lying s states, *viz.*, $1s$ and $2s$. It is worth mentioning at the outset that, henceforth all quantities are given in atomic unit, unless mentioned otherwise. We have carefully selected 14 r_c to cover *small, intermediate and large* range of confinement. As mentioned previously, a host of results for such low states exists. Best six of them are chosen as reference for comparison. For the entire range of radius, energies were computed to seven-figure accuracy in [35]. Exact energies, expressed through Kummer M -functions [34], are also available for these states. For all values of radii, present energies for both states completely agree with the quoted values, for up to the precision they are presented in [34]. Some other very accurate results are also found, e.g., the series method [33], asymptotic

TABLE I: Energies (a.u.) of CHA for low-lying states. PR implies Present Result.

| r_c | E_{1s} (PR) | E_{1s} (Literature) | r_c | E_{2s} (PR) | E_{2s} (Literature) |
|-------|-----------------|--|-------|-----------------|--|
| 0.1 | 468.9930386595 | 468.9930 ^a ,468.9930386593 ^b ,468.99313 ^c | 0.1 | 1942.720354554 | 1942.720 ^a |
| 0.2 | 111.0698588367 | 111.0698588368 ^b ,111.07107 ^c | 0.2 | 477.8516723922 | |
| 0.5 | 14.74797003035 | 14.74797 ^a ,14.74797003035 ^{b,d} ,14.74805 ^c | 0.5 | 72.67203919047 | 72.67204 ^a ,72.67203919046 ^d |
| 1.0 | 2.373990866100 | 2.373991 ^a ,2.373990866103 ^{b,d} , 2.37399 ^c ,2.373990866 ^e | 1.0 | 16.57025609346 | 16.57026 ^a ,16.57025609346 ^d , 16.570256093 ^e |
| 1.5 | 0.437018065247 | 0.437018065247 ^d | 2.0 | 3.327509156489 | 3.327509 ^a ,3.32750915649 ^f |
| 2.0 | -0.125000000002 | -0.1250000 ^a ,-0.125000000000 ^{b,d} , -0.12500 ^c ,-0.125000000 ^e ,-0.12500000000 ^f | 4.0 | 0.420235631712 | 0.4202356 ^a ,0.420235631713 ^d , |
| 3.0 | -0.423967287733 | -0.423967287733 ^{b,d} | 6.0 | 0.012725103091 | 0.01272510 ^a ,0.012725103090 ^d |
| 4.0 | -0.483265302077 | -0.4832653 ^a ,-0.483265302078 ^{b,d} , -0.48327 ^c | 8.0 | -0.084738721360 | -0.08473872 ^a ,-0.0847387213569 ^d , -0.084738721 ^e ,-0.08473872135 ^{f,g} |
| 5.0 | -0.496417006591 | -0.496417006591 ^d | 10.0 | -0.112806210298 | -0.1128062 ^a ,-0.112806210295 ^d , -0.11280621029 ^f ,-0.112806210296 ^g |
| 6.0 | -0.499277286372 | -0.4992773 ^a ,-0.499277286372 ^d , -0.49928 ^c | 14.0 | -0.124015029434 | -0.124015029431 ^d ,-0.124015029 ^e , -0.12401502943 ^f ,-0.124015029432 ^g |
| 8.0 | -0.499975100445 | -0.4999751 ^a ,-0.49997 ^c ,-0.499975100445 ^d , -0.499975100 ^e ,-0.49997510044 ^f , -0.499975100446 ^g | 20.0 | -0.124987114308 | -0.124987114312 ^d ,-0.124987114 ^e , -0.124987114313 ^g |
| 10.0 | -0.499999263281 | -0.4999993 ^a ,-0.50000 ^c ,-0.499999263281 ^d , -0.49999926328 ^f ,-0.499999263282 ^g | 25.0 | -0.124999763707 | -0.1249998 ^a ,-0.12499976370 ^f |
| 12.0 | -0.499999980159 | -0.49999998015 ^f ,-0.499999980159 ^g | 30.0 | -0.124999996469 | -0.12499999646 ^f |
| 20.0 | -0.500000000000 | -0.499999999999 ^d ,-0.500000000 ^e | 40.0 | -0.124999999998 | -0.12499999999 ^g |

^aRef. [35].

^bRef. [32].

^cRef. [55].

^dRef. [33].

^eRef. [34].

^fRef. [24].

^gRef. [29].

iteration method [32]. Former results exist for both states, while same for the latter offers only $2s$ states. For all instances, our energies are seen to either agree completely with these, or differ only in the last place of decimal quoted. Reasonably accurate eigenvalues of these states are also reported for intermediate to large r_c values in [24] and for $r_c \geq 8$ in [29]. Qualitatively correct energies for ground state were obtained from some simple variational wave functions [22], and a variational method with generalized Hylleraas basis set as well as a perturbative approach using exact solution of confined free particles as unperturbed wave function [55]. As seen, energy levels are raised relative to the free-atom values. Obviously, as r_c tends to infinity, eigenvalues monotonically approach the corresponding values of free H atom. With an increase in quantum number n , the required r_c values to attend the energy of unconfined H atom, increases. One also notices that the extent by which a CHA level is raised relative to the free H atom, tends to increase as r_c decreases.

TABLE II: Energies (a.u.) of CHA for low-lying states. PR implies Present Result.

| r_c | E_{2p} (PR) | E_{2p} (Literature) | r_c | E_{3p} (PR) | E_{3p} (Literature) |
|-------|-----------------|--|-------|-----------------|---|
| 0.1 | 991.0075894412 | 991.0076 ^a | 0.1 | 2960.462302278 | 2960.462 ^a |
| 0.2 | 243.1093166600 | | 0.2 | 734.2292278041 | |
| 0.5 | 36.65887588018 | 36.65888 ^a ,36.703 ^b ,36.65887588018 ^c | 0.5 | 114.6435525192 | 114.6436 ^a ,114.6435525192 ^c |
| 1.0 | 8.223138316165 | 8.223138 ^a ,8.233 ^b ,8.223138316160 ^c ,8.232 ^d , 8.223138316 ^e ,8.223138316160 ^f | 1.0 | 27.47399530254 | 27.47400 ^a ,27.47399530253 ^c , 27.473995303 ^e |
| 2.0 | 1.576018785601 | 1.576019 ^a ,1.57775 ^b ,1.576018785606 ^{c,f} , 1.57735 ^d ,1.576018786 ^e ,1.57601878560 ^g | 2.0 | 6.269002791978 | 6.269003 ^a ,6.269002791986 ^c , 6.269002792 ^e |
| 4.0 | 0.143527083713 | 0.1435271 ^a ,0.14366 ^b ,0.143527083713 ^{c,f} , 0.14359 ^d ,0.14352708371 ^g | 5.0 | 0.707718415829 | 0.707718415822 ^c |
| 6.0 | -0.05555555557 | -0.05555556 ^a ,-0.055555 ^{b,d} ,-0.05555555555 ^c | 10.0 | 0.049190760574 | 0.04919076 ^a ,0.049190760586 ^c |
| 8.0 | -0.104450066408 | -0.1044501 ^a ,-0.10441 ^b , -0.104450066406 ^{c,f,h} , -0.104450066 ^e ,-0.10445006640 ^g | 14.0 | -0.027268482516 | -0.027268482486 ^c , -0.027268482 ^e |
| 10.0 | -0.118859544856 | -0.1188595 ^a ,-0.118859544853 ^c , -0.11885954485 ^g ,-0.118859544854 ^h | 20.0 | -0.051611419756 | -0.051611419761 ^c , -0.051611420 ^e |
| 14.0 | -0.124540597991 | -0.124540597990 ^{c,h} ,-124540598 ^e ,-12454059799 ^g | 25.0 | -0.054909464520 | -0.05490946 ^a |
| 20.0 | -0.124994606646 | -124994606647 ^{c,h} ,-0.124994607 ^e ,-0.12499460664 ^g | 30.0 | -0.055471281464 | |
| 25.0 | -0.124999906046 | -0.1249999 ^a ,-0.12499990604 ^g | 40.0 | -0.05554769957 | |
| 30.0 | -0.12499998641 | -0.1249999864 ^g | 50.0 | -0.05555551158 | -0.0555555 ^a |
| 40.0 | -0.12499999999 | | 55.0 | -0.05555555273 | |

^aRef. [35].

^bRef. [27].

^cRef. [33].

^dRef. [21].

^eRef. [34].

^fRef. [32].

^gRef. [24].

^hRef. [29].

Next, Table II offers energies of two low-lying excited states having $\ell = 1$, namely, $2p$ and $3p$, of a CHA for varying radii (at 14 selected) of the enclosure. Once again, a decent number of theoretical results are available for these states, especially in the intermediate r_c ; some of those are duly quoted here for comparison. For the asymptotically small radius ($r_c < 0.5$), only one result could be found; present energies are clearly much better than the reference values [35]. On the other hand, the intermediate- r_c results for $2p$ state are seen to match quite nicely with the algebraic solution of [29]. As in the previous table, current eigenvalues are very much competitive to those of [32–34]; in several occasions completely reproducing the latter ones. For $2p$ state, some intermediate- r_c results were reported through a supersymmetric variational method [27] as well as a variational method [21], offering qualitatively good energies. Free-atom energies are regained back for sufficiently large box size r_c ; large n requires large r_c . Other general conclusions of Table I remain valid here also.

Now Table III offers results on select 12 low- and moderately-high-lying excited states of CHA corresponding to $3 \leq n \leq 5$; $\ell \leq 4$, to establish the efficiency and usefulness

TABLE III: Energies (a.u.) of CHA for some high-lying states. PR implies Present Result.

| State | r_c | Energy (PR) | Energy (Reference) | r_c | Energy (PR) | Energy (Reference) |
|-------|-------|---------------|--|-------|---------------|--|
| 3s | 0.1 | 4406.1216518 | 4406.122 ^a | 1 | 40.863124601 | 40.86312 ^a ,40.863124601 ^{b,c} |
| | 5 | 1.0532206154 | 1.0532206155 ^c | 15 | -0.0268748755 | |
| | 25 | -0.0545924509 | -0.05459245 ^a | 50 | -0.0555555478 | -0.05555555 ^a |
| 4s | 0.1 | 7857.6291849 | 7857.629 ^a | 1 | 75.130493060 | 75.13049 ^a ,75.130493061 ^{b,c} |
| | 5 | 2.3823251868 | 2.3823251868 ^c | 25 | -0.0132027435 | -0.01320274 ^a |
| | 40 | -0.0305518195 | | 50 | -0.0312043375 | -0.03120434 ^a |
| 5s | 0.1 | 12296.731659 | 12296.73 ^a | 1 | 119.32706249 | 119.3271 ^a ,119.327062496 ^{b,c} |
| | 10 | 0.8263888778 | 0.8263889 ^a ,0.8263888778 ^c | 20 | 0.1128777394 | 0.112877739 ^b ,0.1128777394 ^c |
| | 40 | -0.0110593683 | | 60 | -0.0195964955 | |
| 4p | 0.1 | 5918.1828889 | 5918.183 ^a | 1 | 56.758033888 | 56.75803 ^a ,56.758033888 ^b |
| | 5 | 1.8304233586 | | 25 | -0.0165034620 | -0.01650346 ^a |
| | 40 | -0.0307098946 | | 50 | -0.0312164983 | -0.03121650 ^a |
| 5p | 0.1 | 9863.6047594 | 9863.605 ^a | 1 | 95.991853334 | 95.99185 ^a ,95.991853335 ^b |
| | 10 | 0.6883703331 | 0.6883703 ^a | 20 | 0.0951697270 | |
| | 40 | -0.0122109669 | | 60 | -0.0196650907 | |
| 3d | 0.1 | 1644.5299223 | 1644.530 ^a | 1 | 14.967464086 | 14.96746 ^a ,14.9895 ^d ,14.979 ^e |
| | 5 | 0.3291171429 | 0.329425 ^d ,0.329365 ^e | 15 | -0.0466425817 | -0.046635 ^e |
| | 25 | -0.0553214524 | -0.05532145 ^a , -0.05532145239 ^f | 50 | -0.0555555544 | -0.05555555 ^a , -0.0555555544 ^f |
| 4d | 0.1 | 4115.5826320 | 4115.583 ^a | 1 | 39.315319855 | 39.31532 ^a |
| | 5 | 1.2396510218 | | 25 | -0.0218552724 | -0.02185527 ^a |
| | 40 | -0.0309495183 | | 50 | -0.0312333327 | -0.03123333 ^a |
| 5d | 0.1 | 7569.5425196 | 7569.543 ^a | 1 | 73.601919340 | 73.60192 ^a |
| | 10 | 0.5213480960 | 0.5213481 ^a | 20 | 0.0682442940 | |
| | 40 | -0.0142130246 | | 60 | -0.0197771075 | |
| 4f | 0.1 | 2426.3955489 | 2426.396 ^a | 1 | 22.895825482 | 22.89583 ^a |
| | 5 | 0.6694519803 | | 25 | -0.0274353350 | -0.02743534 ^a |
| | 40 | -0.0311568571 | | 50 | -0.0312456821 | -0.03124568 ^a |
| 5f | 0.1 | 5407.2220240 | 5407.222 ^a | 1 | 52.395102963 | 52.39510 ^a |
| | 10 | 0.3525841702 | 0.3525842 ^a | 20 | 0.0384456748 | |
| | 40 | -0.0165731807 | | 60 | -0.0198918442 | |
| 5g | 0.1 | 3333.3040034 | 3333.304 ^a | 1 | 32.034089112 | 32.03409 ^a |
| | 10 | 0.1883418745 | 0.1883419 ^a | 20 | 0.0090019053 | |
| | 40 | -0.0187098818 | | 60 | -0.0199708957 | |
| | 80 | -0.0199997891 | | 100 | -0.0199999992 | |

^aRef. [35].

^bRef. [34].

^cRef. [33].

^dRef. [21].

^eRef. [27].

^fRef. [24].

TABLE IV: Eigenvalues (in a.u.) of $n = 8$ states of 3D CHA as function of r_c .

| ℓ | $r_c = 1$ | $r_c = 25$ | $r_c = 50$ | $r_c = 75$ | $r_c = 100$ | $r_c = 150$ | $r_c = 175$ |
|--------|--------------|-------------|-------------|-------------|-------------|-------------|-------------|
| 0 | 311.32325639 | 0.328725861 | 0.04409216 | 0.00483160 | -0.00466283 | -0.0077439 | -0.0078087 |
| 1 | 273.14306704 | 0.301937308 | 0.04108258 | 0.00416432 | -0.00484461 | -0.0077505 | -0.0078091 |
| 2 | 235.92204657 | 0.264080555 | 0.03584294 | 0.00292353 | -0.00518755 | -0.0077624 | -0.0078098 |
| 3 | 199.97204134 | 0.222512230 | 0.02927280 | 0.00125898 | -0.00565391 | -0.0077768 | -0.0078107 |
| 4 | 165.32153876 | 0.180052301 | 0.02204074 | -0.00066615 | -0.00619372 | -0.0077909 | -0.0078115 |
| 5 | 131.87629255 | 0.137914527 | 0.01458520 | -0.00269811 | -0.00674844 | -0.0078021 | -0.0078120 |
| 6 | 99.330037127 | 0.096520395 | 0.00718594 | -0.00469286 | -0.00725165 | -0.0078089 | -0.0078123 |
| 7 | 66.624595253 | 0.055270190 | -0.00001574 | -0.00649140 | -0.00762894 | -0.0078118 | -0.0078124 |

of our present method in confined situations. In all cases, a wide region of confinement has been considered. Unlike the previous tables, in this case, reference results are rather scarce, which are quoted appropriately. For all these states, some results are available from the numerical calculation of [35], showing a decent agreement with ours. For s , p states, best reference energies are those from [24] and [34]; gratifyingly, present eigenvalues are in excellent agreement with these. For d series, best literature energies seem to be those reported in [24]; here also one notices good matching between present and literature values. No reference values other than those in [35] could be found for the $\ell > 2$ series for comparison. As seen, in all cases, present results are significantly improved from the reference ones. For $3d$ states of CHA, reasonably good energies are also reported in the variational [21] and super-symmetric [27] calculation. As can be seen, many of these states have not been reported earlier, especially for medium and large r_c . Given the success of this method for all the states reported before, we are confident that these are also equally accurate; they may constitute a useful reference for future investigations on such systems.

Once the low-lying states of Tables I, II and III are obtained, an extension is made for some high-lying excited states, as a further illustration of feasibility and performance of the approach. As a representative set, all 8 states belonging to $\ell = 0 - 7$ corresponding to $n = 8$ of CHA are tabulated in Table IV. Higher states have been scarcely dealt in literature; thus no references exist. Eigenvalues for all these are given at seven selected r_c values, namely, 1, 25, 50, 75, 100, 150, 175 a.u. to cover a broad region of confinement. Within a particular n , for a fixed r_c , energies are split such that, with increase in ℓ , the latter decreases, so that the sub-level with *largest* ℓ corresponds to *lowest* energy. Obviously, as $r_c \rightarrow \infty$, all states regain the free-atom energies. A careful examination of the above tables

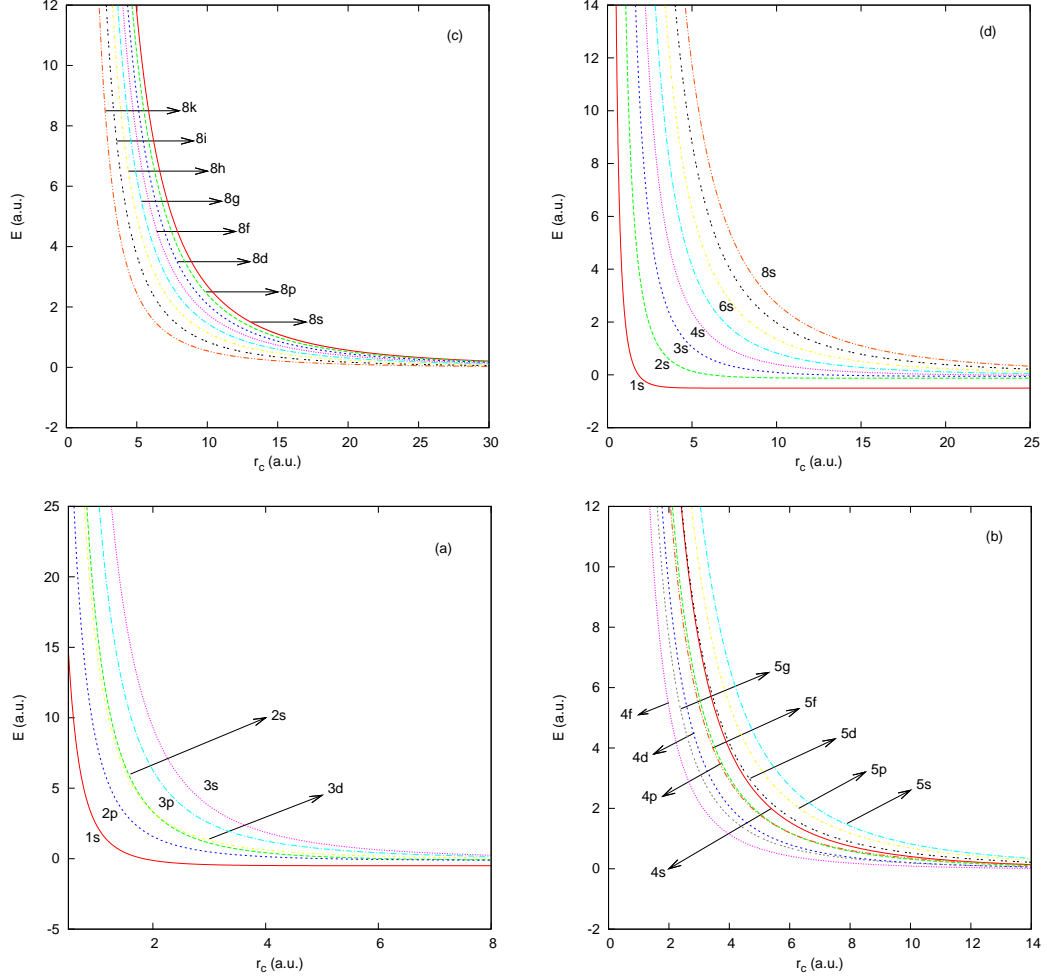


FIG. 1: Energy variations in CHA with r_c : (a) 6 states corresponding to $n = 1, 2, 3$ (b) 9 states with $n = 4, 5$ (c) Eight $n = 8$ states having $\ell = 0 - 7$ (d) Eight $\ell = 0$ states having $n = 1 - 8$.

reveals that, for a given r_c , the extent by which a particular level is raised with respect to its corresponding free state, is relatively less for ground state compared to excited state; generally increasing with n for a specific ℓ . For example, the magnitude of the shift in energy from its unconfined counterpart, $\Delta E_{nl}^{r_c} = E_{nl}^{r_c} - E_{nl}$, for $1s$ are: 1.4×10^{-4} , 2.5×10^{-5} , 7.4×10^{-7} , 2.0×10^{-8} , 5.0×10^{-10} , for $r_c = 7, 8, 10, 12, 14$ respectively, while the same values for $2s$ are: 7.4×10^{-2} , 4.0×10^{-2} , 1.2×10^{-2} , 3.6×10^{-3} , 9.8×10^{-4} . These differences decrease in an exponential fashion with increasing r_c and then finally vanish for a wall placed at sufficiently large distance; which is consistent with the findings of [29, 31]. It is hoped that, in future, these results would be helpful for calibration of other methods.

Above energy variations of CHA in Tables I–IV are graphically shown in Fig. 1 for medium to large-size cavity. Note that, ranges of r_c and energy axes are different for different plot.

Also in all the cases, confinement in very small-sized box is ignored as this gives rise to very high energy values making the plots difficult to visualize. Panels (a), (b) depict energies of all six ($1s, 2s, 2p, 3s, 3p, 3d$) states corresponding to $n = 1 - 3$ and all nine states for $n = 4, 5$ respectively, with changes in r_c . It is well-known that the characteristic *accidental* degeneracy of free H atom (a consequence of the central Coulombic field), is broken in presence of a hard impenetrable wall at *all* finite radius r_c . This is due to the fact that confinement results in a violation of the requirement of the potential being purely Coulombic everywhere. The adjacent plots remain parallel to each other. General nature of the plots are consistent with those of a central potential under an isotropic confinement, i.e., very high energy at small r_c followed by a sharp decline with an increase in r_c , finally attaining the value of that of respective free atom at a sufficiently large r_c and remaining constant afterwards. In all cases, individual confined energy levels are raised relative to the unconfined H case. For a given state, the magnitude by which this raise occurs, increases as r_c assumes progressively smaller values. This is promptly verified from the $\Delta_{n\ell}^{r_c}$ values, as defined earlier, for example, for $2p$ state, as in the sequence: $6.9 \times 10^{-2}, 6.1 \times 10^{-3}, 2.3 \times 10^{-4}, 5.4 \times 10^{-6}, 9.4 \times 10^{-8}, 1.4 \times 10^{-9}$, corresponding to r_c values of 6, 10, 15, 20, 25, 30 respectively. Such a system is also known to exhibit *simultaneous degeneracy*, whereby, for all $n \geq \ell + 2$, a CHA state characterized by quantum numbers (n, ℓ) becomes degenerate to a $(n + 1, \ell + 2)$ state, exactly at $r_c = (\ell + 1)(\ell + 2)$. Thus it is seen that $2s$ and $3d$ states are degenerate at $r_c = 2$. Some other similar pairs are $(4s, 5d)$ at $r_c = 2$, as well as $(3s, 4d)$, $(3p, 4f)$, $(4p, 5f)$, all at $r_c = 6$. Panel (c) displays all the eight states (having $\ell = 0 - 7$) corresponding to $n = 8$ as in Table IV. Within a given n , the sub- ℓ levels do not cross each other; all the plots remain well-separated at small r_c and gradually reaches the free-atom value at large r_c . As r_c decreases, higher- ℓ states get relatively more stabilized such that, for a particular r_c , accidental degeneracy breaks down to make the highest- ℓ state lowest in energy and vice versa [37]. Therefore, for a particular n , one finds inequalities such as: $E_{2p} < E_{2s}$; $E_{3d} < E_{3p} < E_{3s}$; $E_{4f} < E_{4d} < E_{4p} < E_{4s}$, etc. Lastly in (d) is shown the plots for eight s -waves ($\ell = 0$) having radial quantum numbers $n = 1 - 8$. Here also, the plots remain well-separated and monotonically decreasing with increase in r_c . For a given ℓ and r_c , state with lowest n remains lowest in energy and vice versa. Similar pattern has been found for other ℓ values and omitted therefore. As expected, as the cavity size becomes smaller, many complex energy splitting is observed, especially with higher n, ℓ quantum numbers. We have

TABLE V: Estimated critical cage radius r_c^c (a.u.) of CHA. All states having $n = 1 - 10$ are given.

| n | State | | | | | | | | | |
|-----|---------------------------|---------------------------|---------------------|---------------------|---------------------|---------------------|---------------------|---------------------|---------------------|---------------------|
| | s | p | d | f | g | h | i | k | l | m |
| 1 | 1.8352463302 | | | | | | | | | |
| | 1.8352463302 ^a | | | | | | | | | |
| 2 | 6.152307040 | 5.0883082272 | | | | | | | | |
| | 6.152307040 ^a | 5.0883082272 ^a | | | | | | | | |
| 3 | 12.93743173 | 11.90969656 | 9.6173660416 | | | | | | | |
| | 12.93743173 ^a | 11.90969656 ^a | 9.6174 ^b | | | | | | | |
| 4 | 22.19009585 | 21.1744312 | 19.03014422 | 15.36345002 | | | | | | |
| | 22.19009585 ^a | 21.1744312 ^a | 19.030 ^b | 15.363 ^b | | | | | | |
| 5 | 33.9102067 | 32.900106 | 30.8119332 | 27.4587506 | 22.2921676 | | | | | |
| | 33.9102067 ^a | 32.900106 ^a | 30.812 ^b | 27.459 ^b | 22.292 ^b | | | | | |
| 6 | 48.097738 | 47.090674 | 45.030686 | 41.80445 | 37.15745 | 30.380418 | | | | |
| | 48.097738 ^a | 47.090674 ^a | 45.031 ^b | 41.805 ^b | 37.157 ^b | 30.380 ^b | | | | |
| 7 | 64.752680 | 63.747462 | 61.703830 | 58.54454 | 54.11667 | 48.09827 | 39.61139 | | | |
| | 64.753 ^b | 63.747459 ^a | 61.704 ^b | 58.545 ^b | 54.117 ^b | 48.098 ^b | 39.611 ^b | | | |
| 8 | 83.874996 | 82.87098 | 80.83777 | 77.71881 | 73.41012 | 67.72065 | 60.2595 | 49.9721 | | |
| | 83.875 ^b | 82.871 ^b | 80.838 ^b | 77.719 ^b | 73.410 ^b | 67.721 ^b | 60.260 ^b | 49.972 ^b | | |
| 9 | 105.466510 | 104.46246 | 102.43536 | 99.3425 | 95.1077 | 89.6012 | 82.5940 | 73.6240 | 61.452 | |
| | 105.46 ^b | 104.46 ^b | 102.44 ^b | 99.343 ^b | 95.108 ^b | 89.601 ^b | 82.594 ^b | 73.624 ^b | 61.452 ^b | |
| 10 | 129.49108 | 128.5179 | 126.5288 | 123.4622 | 119.2614 | 113.8539 | 107.0970 | 98.718 | 88.177 | 74.044 |
| | 129.52 ^b | 128.52 ^b | 126.50 ^b | 123.42 ^b | 119.24 ^b | 113.85 ^b | 107.10 ^b | 98.718 ^b | 88.178 ^b | 74.045 ^b |

^aref. [32].

^bref. [52].

found the energy orderings for CHA in the limit of $r_c \rightarrow 0$ as,

$$1s, 2p, 3d, 2s, 4f, 3p, 5g, 4d, 6h, 3s, 5f, 7i, 4p, 8k, 6g, 5d, 4s, 9l, 7h, 6f, 10m, 5p, 8i, \dots$$

It is noticed that as one goes to higher levels, there is significant intermixing between levels belonging to different n values. This arises presumably due to the fact that as confining radius decreases, there is a lot of crossover between levels of different n, ℓ values.

Now the attention is turned to *zero-energy* case, i.e., estimation of the minimum cavity radius that can accommodate a bound state in a CHA. As apparent from our above discussion, binding energy of a CHA gradually diminishes with reduction in the size of cavity, rendering all states to have positive energy at sufficiently small r_c . Thus it is of importance to find out the cavity radius at which the binding energy becomes zero, the so-called *critical cage radius*, r_c^c . For example, these have relevance in the study of partition function of atomic H as well as in the ionization of ground and excited state. Table V reports our calculated

critical values for all 55 eigenstates of CHA, starting from ground state $1s$ to $10m$. Its first calculation for ground state of CHA produced a value of 1.835 a.u., which was reported as early as in 1938 in the work of [9], through the zeros of Bessel's function of first kind of order p , $J_p(z)$. Thereafter, a slightly better value (1.8354) was presented in [69]. Some authors [11] also showed the ionization cage radii to be proportional to the zeros of Bessel functions. However, the first systematic investigation on all states up to and belonging to $n = 10$ were undertaken by [52] through a variational calculation, which are duly quoted here for comparison. There, five significant-figure accurate results were given; current GPS results are considerably improved, especially for lower states. Results for first 6 states corresponding to $\ell = 0, 1$ show *complete* agreement with the accurate asymptotic iteration result [32] for all but $7p$ state. First five states of $\ell = 0, 1$ are also available from precise calculations of [34], which again corroborate our present critical radii values. Estimation of these become progressively more difficult for higher n, ℓ quantum numbers, due to complex mixing amongst states. In general, for a given n , critical radius tends to increase with ℓ , while for a fixed ℓ , the same decreases as n increases. Furthermore, the disappearance of degeneracy in energy levels with respect to ℓ quantum number for a given n in CHA is reminiscent to that of the effect of *screening* on energy levels in a Coulomb potential [59], e.g., a Hulthén or Yukawa potential. It is well-known that in case of a *screened* Coulomb potential, bound states exist only for certain values of screening parameter below a threshold limit; if the parameter goes beyond this critical value, the state becomes unbound. Analogously, for H atom, under the influence of spherical confinement, a level becomes unbound if the confining radius remains below the critical cage radius, and bound otherwise.

As a further verification on the accuracy and faithfulness of our calculation, Table VI, additionally presents selected radial expectation values, *viz.*, $\langle r^{-2} \rangle$, $\langle r^{-1} \rangle$, $\langle r \rangle$, and $\langle r^2 \rangle$ of CHA. For this, $1s$ and $3d$ are chosen as representative states. The density moments have been reported earlier by many researchers; here the two best results are quoted. The overall qualitative agreement between present result and reference is quite good, again confirming the correctness and accuracy in our wave functions. Like the energy eigenvalues, position expectation values also monotonically approach the corresponding values of free H atom as the box radius tends to infinity. For some of them, no results could be found for comparison.

TABLE VI: Selected expectation values (a.u.), for some low-lying states in CHA.

| State | r_c | $\langle r^{-2} \rangle$ | $\langle r^{-1} \rangle$ | $\langle r \rangle$ | $\langle r^2 \rangle$ |
|-------|-------|--------------------------|----------------------------|-----------------------------|-----------------------------|
| 1s | 0.5 | 40.6912615553 | 5.11404400581 | 0.242490864909 | 0.067128353708 |
| | | | 5.11404400581 ^a | | |
| 3d | 2.0 | 11.5924623961 | 3.28244199632 | 0.322576865990 | 0.108950015348 |
| 1s | | 4.10532919705 | 1.53516170643 | 0.859353174267 | 0.874825394135 |
| 3d | 10.0 | 0.749825224105 | 1.53516170643 ^a | 0.859353174266 ^a | 0.874825394134 ^a |
| | | | 0.832951857503 | 1.27525204948 | 1.70676316887 |
| 1s | 10.0 | 1.99993975471 | 0.832952 ^b | 1.275252 ^b | 1.706763 ^b |
| | | | 1.00001169282 | 1.49993637877 | 2.99945950887 |
| 3d | 10.0 | 0.038607686219 | 1.00001169282 ^a | 1.49993637877 ^a | 2.999459508865 ^a |
| | | | 0.185997997884 | 5.84705927624 | 36.5172404570 |

^aRef. [33].

^bRef. [26].

B. Confined Hulthén Potential

As an attempt to assess and extend the domain of applicability of our scheme to other Coulombic systems, at this stage, the focus is shifted to the case of spherical confinement for the familiar short-range Hulthén potential. It may be noted that, while many high-quality results are available for confined H atom, same for other Coulombic systems are rather scarce. Some notable confinement works along this direction include (a) Hulthén potential [17, 28, 70–72] (b) Coulomb plus harmonic oscillator [73, 74] (c) Morse potential [75] (d) Lennard-Jones potential [76], etc. Since maximum work has been done on (a), it is selected here to facilitate easy comparison. This potential shows Coulomb-like behavior for small r and decays monotonically exponentially to zero for large r . However, interestingly, due to the presence of a screening parameter, it supports only a *limited* number of bound states (unlike the Coulomb potential which possesses infinite number of states) for up to certain values of the parameter below a threshold limit. Furthermore, $\ell = 0$ states of the *free* system offer analytical solutions. Note that, a considerable amount of works exist for the free system. For example, quite accurate energies have been reported by a number of researchers [60, 77–79], which are characterized by complex level crossings for higher quantum numbers.

Tables VII and VIII give sample eigenvalues for two low-lying nodeless states corresponding to $\ell = 0, 1$, *viz.*, $1s, 2p$ of confined Hulthén potential for $\delta = 0.1$ and 0.2 respectively. In both cases, position of the spherical wall was selected at 12 different locations, so as to

TABLE VII: Comparison of some low-lying states of confined Hulthén potential with literature data, for $\delta = 0.1$. PR implies Present Result.

| r_c | E_{1s} (PR) | E_{1s} (Ref.) | E_{2p} (PR) | E_{2p} (Ref.) |
|-------|----------------|---|----------------|--|
| 0.1 | 469.042997232 | | 991.057540215 | |
| 0.5 | 14.7977679573 | | 36.7086314074 | |
| 1.0 | 2.4236006207 | | 8.27265368859 | |
| 1.5 | 0.48645575356 | | 3.28033126465 | |
| 2.0 | -0.07571601608 | -0.07570 ^a , -0.07584 ^b | 1.62506812609 | |
| 6.0 | -0.45051125895 | -0.45035 ^a , -0.45053 ^{b, e} , -0.45109 ^c , -0.44945 ^d | -0.0081227650 | -0.00812 ^a , -0.00815 ^b , -0.00294 ^c , -0.00808 ^d , -0.00865 ^e , -0.00782 ^f |
| 8.0 | -0.45122399716 | -0.45118 ^a , -0.45122 ^{b, e} , -0.45193 ^c , -0.45076 ^d | -0.05762842270 | -0.05762 ^{a, d} , -0.05764 ^b , -0.05293 ^c , -0.05783 ^e , -0.05510 ^f |
| 10.0 | -0.45124920877 | -0.45124 ^a , -0.45125 ^{b, e} , -0.45179 ^c , -0.45098 ^d | -0.0724869919 | -0.07247 ^a , -0.07250 ^b , -0.07008 ^c , -0.07243 ^d , -0.07257 ^e , -0.07196 ^f |
| 15.0 | -0.45124999990 | -0.45125 ^{a, b} | -0.07888401652 | -0.07885 ^a , -0.07888 ^b |
| 25.0 | -0.45125000000 | -0.45125 ^{a, b, d, e} , -0.45131 ^c | -0.07917921743 | -0.07916 ^a , -0.07918 ^{b, e} , -0.07920 ^c , -0.07915 ^d , -0.07921 ^f |
| 40.0 | -0.45124999999 | | -0.07917943910 | -0.07918 ^{a, b} |
| 50.0 | -0.45124999999 | -0.45126 ^c , -0.45125 ^{d, e} | -0.07917943910 | -0.07918 ^{a, b, d, e} , -0.07920 ^{c, f} |

^aRef. [71]. ^bExact result, quoted in [71]. ^cRef. [70]. ^dRef. [28]. ^eExact result, quoted in [28]. ^fRef. [17].

cover *small, intermediate and large* range of confinement. The lowest cavity radius so far considered in literature is: $r_c < 2$ (in case of $1s$, for both δ) and 6 (in case of $2p$, for both δ). Current energies show decent agreement with super-symmetric result of [71] for all values of box size for both states, wherever those are available. The same author also estimated these states by a numerical method that employed Numerov's method with a logarithmic mesh for solution of Schrödinger equation. The latter shows slightly better agreement than super-symmetric result, especially in the neighborhood of *critical cage radius*, r_c^c . This is defined as the radius of the enclosure at which energy becomes zero, analogous to CHA. We have not attempted a detailed study. Rather a more restrictive approach is adopted by estimating a few limited ones. Thus, numerically obtained values of these for $1s, 2p$ states are: 1.8639458, 1.8939725, 1.9584319 and 5.4189704, 5.8257603, 7.0428492 respectively, for $\delta = 0.05, 0.1$ and 0.2. These are in good accord with reported values of 1.894 ($\delta = 0.1$), 1.958 ($\delta = 0.2$) and 5.826 ($\delta = 0.1$), 7.043 ($\delta = 0.2$) for the same states corresponding to screening parameters given in parentheses [71]. In another estimate [72], r_c values are found to be 1.894, 1.958 (for $1s$ state having $\delta = 0.1, 0.2$ respectively), whereas for $2p$ state, the

TABLE VIII: Comparison of some low-lying states of confined Hulthén potential with literature data, for $\delta = 0.2$. PR implies Present Result.

| r_c | $E_{1s}(\text{PR})$ | $E_{1s}(\text{Ref.})$ | $E_{2p}(\text{PR})$ | $E_{2p}(\text{Ref.})$ |
|-------|---------------------|---|---------------------|--|
| 0.1 | 469.092872952 | | 991.107392541 | |
| 0.5 | 14.8471617711 | | 36.7578980396 | |
| 1.0 | 2.4724301161 | | 8.32120019501 | |
| 1.5 | 0.53476949305 | | 3.32817211249 | |
| 2.0 | -0.02786272697 | -0.02784 ^a , -0.02800 ^b | 1.67221901970 | |
| 6.0 | -0.40421171842 | -0.40404 ^a , -0.40423 ^b | 0.03422237169 | |
| 8.0 | -0.40497046759 | -0.40493 ^a , -0.40497 ^b | -0.01709196413 | -0.01709 ^a , -0.01710 ^b , -0.01242 ^c , -0.01708 ^d , -0.01607 ^e , -0.01731 ^f |
| 10.0 | -0.40499902640 | -0.40499 ^a , -0.40500 ^b | -0.0332989638 | -0.03329 ^a , -0.03330 ^b , -0.03118 ^c , -0.03323 ^d , -0.03389 ^e , -0.03339 ^f |
| 15.0 | -0.40499999985 | -0.40499 ^a , -0.40500 ^b | -0.04128265021 | -0.04125 ^a , -0.04128 ^b |
| 25.0 | -0.40499999999 | -0.40500 ^{a, b} | -0.04188395482 | -0.04188 ^{a, b, f} , -0.04199 ^c , -0.04178 ^d , -0.04192 ^e |
| 40.0 | -0.40499999999 | | -0.04188604888 | -0.04188 ^a , -0.04189 ^b |
| 50.0 | -0.40499999999 | | -0.04188604921 | -0.04189 ^{a, b, d, f} , -0.04196 ^c , -0.04191 ^e |

^aRef. [71]. ^bExact result, quoted in [71]. ^cRef. [70]. ^dRef. [28]. ^eRef. [17]. ^fExact result, quoted in [28].

corresponding values are 5.826 and 7.043. Excepting $\delta = 0.2$ of $1s$, other three cases were studied by $1/N$ expansion method [70]. One notices that, generally, as r_c goes to higher values, these results tend to improve. For some three cases, energies were reported by supersymmetric variational method [28] and WKB method [17], leading to quite similar accuracy and conclusions as those in [70]. Numerical estimates, as quoted in [28], are also produced wherever possible. While these reference energies show good agreement with each other, present values are considerably more accurate than all of these.

Next, Table IX presents calculated energies of Hulthén potential under spherical confinement for some representative moderately high-lying states. As an illustration, the screening parameter is fixed at $\delta = 0.05$ and seven states are chosen corresponding to $n = 3, 4$, at ten selected values of r_c , *viz.*, 0.1, 0.5, 1, 2, 5, 10, 20, 30, 50 and 100 a.u., respectively. In each case, energy, much like the case of CHA, steadily decreases from a high positive value to attain a negative value for a sufficiently high r_c and remains stationary thereafter. Full confinement region is scanned. To the best of our knowledge, no such attempt is known for such states and they may offer a useful set of reference for future works in this direction.

We graphically show the effect of isotropic compression on energies of Hulthén potential

TABLE IX: Eigenvalues (a.u.) of $n = 3, 4$ states of confined Hulthén potential for $\delta = 0.05$.

| State | $r_c = 0.1$ | $r_c = 0.5$ | $r_c = 1$ | $r_c = 2$ | $r_c = 5$ |
|-------|--------------|---------------|---------------|--------------|--------------|
| 3s | 4406.1466414 | 170.61011193 | 40.888019695 | 9.3389386065 | 1.0776696979 |
| 3p | 2960.4872910 | 114.66849642 | 27.498883279 | 6.2937792870 | 0.7321605002 |
| 3d | 1644.5549089 | 63.185117264 | 14.992330190 | 3.3522434990 | 0.3534709790 |
| 4s | 7857.6541745 | 308.22219525 | 75.155388308 | 17.840882601 | 2.4067849721 |
| 4p | 5918.2078780 | 232.45290563 | 56.782925033 | 13.535366380 | 1.8548769549 |
| 4d | 4115.6076200 | 161.38194690 | 39.340200641 | 9.3389126846 | 1.2640613859 |
| 4f | 2426.4205347 | 94.651526411 | 22.920683088 | 5.3668108085 | 0.6937529695 |
| | $r_c = 10$ | $r_c = 20$ | $r_c = 30$ | $r_c = 50$ | $r_c = 100$ |
| 3s | 0.1152515762 | -0.0272469617 | -0.0331906519 | -0.033368031 | -0.033368055 |
| 3p | 0.0730498617 | -0.0288228707 | -0.0330474388 | -0.033164486 | -0.033164501 |
| 3d | 0.0166906839 | -0.0309487936 | -0.0327122864 | -0.032753179 | -0.032753184 |
| 4s | 0.4290276270 | 0.0393206209 | -0.003319140 | -0.011126878 | -0.011249999 |
| 4p | 0.3399459526 | 0.0307423709 | -0.0045189174 | -0.010961108 | -0.011058170 |
| 4d | 0.2262751307 | 0.0171189105 | -0.0064514215 | -0.010611090 | -0.010667404 |
| 4f | 0.1118826554 | 0.0024927744 | -0.0083336240 | -0.010043093 | -0.010061964 |

in Fig. 2 now. In left side (a), these are given for all six states corresponding to $n = 1 - 3$ having, $\delta = 0.2$, while right side (b) considers all nine states belonging to $n = 4, 5$ with screening parameter 0.05 respectively. In both occasions, positive and negative energies are included. Shapes of all these curves are quite similar to each other. Note the axes of energy and box radius are different in two cases. Confinement within very small box size is again avoided for easy appreciation of figures. They all exhibit a sharp increase as r_c becomes smaller. Plots remain well separated at relatively smaller r_c . From an initial high positive value, they fall off rapidly monotonically as r_c increases, finally approaching the energy of corresponding free system smoothly and remaining constant thereafter. As r_c decreases, energies change sign from negative to positive values becoming zero for critical cavity radius. Like the case of Coulomb potential, for a given δ and r_c , state with *lowest* n remains lowest in energy within a particular ℓ , whereas, for a given n , state with *highest* ℓ corresponds to lowest energy. Furthermore, for a specific δ , sequence of energy follows the *same* pattern as Coulomb potential of previous section in the limit of $r_c \rightarrow 0$. However, the same in unconfined case is as follows:

$$1s, 2s, 2p, 3s, 3p, 3d, 4s, 4p, 4d, 4f, 5s, 5p, 5d, 5f, 5g, 6s, 6p, 6d, 6f, 6g, \dots$$

Finally, a few words about the dipole polarizability of confined Hulthén potential. The exact calculation of polarizability is quite involved; we use simplified expressions, originally

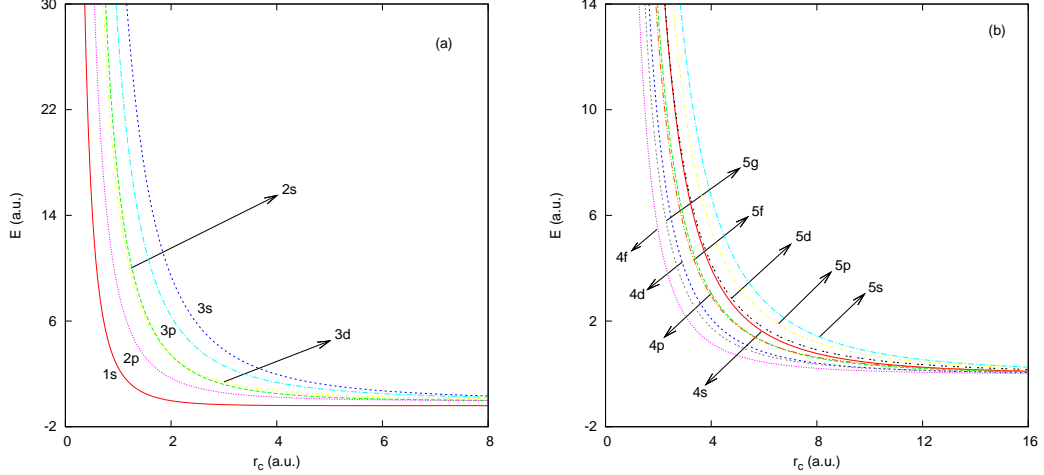


FIG. 2: Energy variations in Hulthén potential with confinement radius: (a) $n = 1, 2, 3$ (b) $n = 4, 5$. Corresponding δ values are 0.2 and 0.05 for (a), (b). See text for details.

derived for one-electron atoms in free-space, by Kirkwood [80] and Buckingham [81], namely,

$$\alpha_D^K = \frac{4}{9} \langle r^2 \rangle^2; \quad \alpha_D^B = \frac{2}{3} \left[\frac{6 \langle r^2 \rangle^3 + 3 \langle r^3 \rangle^2 - 8 \langle r \rangle \langle r^2 \rangle \langle r^3 \rangle}{9 \langle r^2 \rangle - 8 \langle r \rangle^2} \right] \quad (5)$$

Assuming that these expressions hold good for confined systems, as has been done in many previous occasions, we summarize our results in Table X. Since a number of high-quality estimates are available for CHA problem (see, for example, [24, 33, 39, 42]), we do not attempt those here and restrict ourselves to the Hulthén potential case. Thus, α_D^K and α_D^B are offered for $1s$ and $2p$ states corresponding to $\delta = 0.1, 0.2$ respectively. In both states, r_c values are chosen so as to cover a broad range. Some results are reported [71] for ground state, which are duly quoted for comparison. No results could be found for excited state. For a given δ , both α_D^K and α_D^B gradually increase with r_c , finally reaching an asymptotic value. For a given δ , one finds that, $\alpha_D^K \leq \alpha_D^B$. Although the inequality holds for free H atom, there is no proof that the same is valid for CHA or a confined Hulthén potential. As r_c increases, difference between the two α tends to increase significantly. It is generally found that polarizability values for $2p$ states are much higher compared to the ground state for a given δ ; moreover, the asymptotic value is reached for a considerably large r_c for $2p$ state. Furthermore, one notices an increase in both α_D^K and α_D^B values with an increase in δ . Present results are significantly improved over the previous ones.

TABLE X: Dipole polarizability (in a.u.) of confined Hulthén potential with respect to cage radius. Numbers in the parentheses denote reference values, taken from [71].

| State | r_c | $\delta = 0.1$ | | $\delta = 0.2$ | |
|-------|-------|--------------------|--------------------|--------------------|--------------------|
| | | α_D^K | α_D^B | α_D^K | α_D^B |
| 1s | 0.5 | 0.002002769 | 0.002030037 | 0.002002790 | 0.002030059 |
| | 1.0 | 0.028478053 | 0.028675462 | 0.028480610 | 0.028678122 |
| | 1.5 | 0.125863099 | 0.126135536 | 0.125903929 | 0.126177170 |
| | 2.0 | 0.340234836(0.340) | 0.340249553(0.340) | 0.340512990(0.340) | 0.340528358(0.340) |
| | 3.0 | 1.17445441(1.175) | 1.18214819(1.183) | 1.17798124(1.180) | 1.18562199(1.188) |
| | 4.0 | 2.29626217(2.29) | 2.36328371(2.35) | 2.31263673(2.31) | 2.37966765(2.37) |
| | 5.0 | 3.21734552(3.18) | 3.41693628(3.36) | 3.25748090(3.24) | 3.45908008(3.41) |
| | 6.0 | 3.72673722(3.67) | 4.07085354(3.97) | 3.79120326(3.77) | 4.14280842(4.08) |
| | 8.0 | 4.00387282(3.93) | 4.48772555(4.36) | 4.09197277(4.06) | 4.59462306(4.51) |
| | 10.0 | 4.02860091(4.00) | 4.53399268(4.48) | 4.12069600(4.09) | 4.64835736(4.59) |
| 2p | 0.5 | 0.003785194 | 0.004204328 | 0.003785213 | 0.004204351 |
| | 3.0 | 4.12373508 | 4.45692552 | 4.12892415 | 4.46314848 |
| | 5.0 | 26.5905910 | 28.0822696 | 26.7681022 | 28.2858721 |
| | 8.0 | 121.326555 | 124.109261 | 125.295494 | 128.358067 |
| | 10.0 | 215.812725 | 217.508104 | 230.776712 | 232.925530 |
| | 15.0 | 395.035988 | 395.743476 | 482.306562 | 483.118500 |
| | 20.0 | 434.150727 | 437.616438 | 578.351678 | 586.056324 |
| | 25.0 | 437.322406 | 441.343442 | 595.270889 | 606.401640 |
| | 30.0 | 437.477603 | 441.540161 | 597.272379 | 609.068736 |

IV. CONCLUSION

Accurate eigenfunctions, energies, radial expectation values are reported for two simple Coulombic systems, namely, H atom and Hulthén potential confined at the center of an impenetrable spherical cavity of radius r_c . The GPS procedure employed here, is able to offer high-quality results (energies correct up to eleven decimal place) uniformly for the *entire* (small, intermediate and large) ranges of confinement. Results for low and higher states are obtained with equal ease and efficiency without necessitating any extensive algebraic manipulation, unlike some other methods. Effects of box radius on energy levels of enclosed system are examined systematically. Present results show, comparable agreement with best theoretical estimates. Critical cavity radii for all states up to and including $n = 10$ for CHA, have been examined. These have been studied by only few workers until now and could be helpful in future. For many states, previous results are significantly improved. The degeneracy breaking as well as energy ordering under the influence of confinement are

also discussed. A similar kind of analysis, as for the CHA, has been made for the latter. In all cases, present results are noticeably superior to all other existing values. Changes of critical screening parameter with respect to confinement radius is briefly discussed. For the latter potential, accurate dipole polarizabilities are provided as well. Considering the simplicity and accuracy offered by this method, it may be also successful and useful for other confinement situations in quantum mechanics.

V. ACKNOWLEDGMENT

Critical constructive comments and suggestions from two kind anonymous referees and the Editor have significantly improved the manuscript. I sincerely thank Prof. N. A. Aquino for kindly supplying a copy of the reference [55]. I am indebted to Prof. K. D. Sen for introducing me in this fascinating area. It is a pleasure to thank Prof. Raja Shunmugam for extending valuable support. The help of our Librarian, Mr. Siladitya Jana, is acknowledged, who procured a few references. Mr. Shahid Ali Farooqui and Mr. Sanjib Das is thanked for their assistance in the figure.

-
- [1] A. Michels, J. de Boer and A. Bijl, *Physica* **4**, 981 (1937).
 - [2] F. M. Fernández and A. Castro, *Kinam.* **4**, 193 (1982).
 - [3] P. O. Fröman, S. Yngve and N. J. Fröman, *J. Math. Phys.* **28**, 1813 (1987).
 - [4] W. Jaskólski, *Phys. Rep.* **271**, 1 (1996).
 - [5] J. P. Connerade, V. H. Dolmatov and P. A. Lakshmi, *J. Phys. B* **33**, 251 (2000).
 - [6] A. L. Buchachenko, *J. Phys. Chem. A* **105**, 5839 (2001).
 - [7] J. Gravesen, M. Willatzen and L. L. Y. Voon, *Phys. Scr.* **72**, 105 (2005).
 - [8] W. D. Heiss (Ed.) *Quantum Dots: A Doorway to Nanoscale Physics*, Springer, Berlin (2005).
 - [9] A. Sommerfeld and H. Welker, *Ann. Phys.* **32**, 56 (1938).
 - [10] T. Guillot, *Planet Space Sci.* **47**, 1183 (1999).
 - [11] S. R. de Groot and C. A. ten Seldam, *Physica* **12**, 669 (1946); *ibid.*, **18**, 891 (1952).
 - [12] D. Suryanarayana and J. A. Weil, *J. Chem. Phys.* **64**, 510 (1976).
 - [13] E. V. Ludeña, *J. Chem. Phys.* **66**, 468 (1977).

- [14] R. Vawter, *J. Math. Phys.* **14**, 1846 (1973).
- [15] V. C. Aguilera-Navarro, E. Ley-Koo and A. H. Zimmerman, *J. Phys. A* **13**, 3585 (1980).
- [16] G. A. Arteca, S. A. Maluendes, F. M. Fernández and E. A. Casttro, *Int. J. Quant. Chem.* **24**, 169 (1983).
- [17] A. Sinha, *J. Math. Chem.* **34**, 201 (2003).
- [18] F. M. Fernández and E. A. Castro, *J. Math. Phys.* **23**, 1103 (1982).
- [19] J. L. Marin and S. A. Cruz, *Am. J. Phys.* **59**, 931 (1991).
- [20] J. L. Marin and S. A. Cruz, *J. Phys. B* **24**, 2899 (1991).
- [21] Y. P. Varshni, *J. Phys. B* **30**, L589 (1997).
- [22] Y. P. Varshni, *Phys. Lett. A* **252**, 248 (1999).
- [23] A. Palma and G. Campoy, *Phys. Lett. A* **121**, 221 (1987).
- [24] N. Aquino, *Int. J. Quant. Chem.* **54**, 107 (1995).
- [25] J. Garza, R. Vargas and A. Vela, *Phys. Rev. E* **58**, 3949 (1998).
- [26] H. E. Montgomery Jr. *Int. J. Mol. Sc.* **2**, 103 (2001).
- [27] E. D. Filho and R. M. Ricotta, *Phys. Lett. A* **299**, 137 (2002).
- [28] E. D. Filho and R. M. Ricotta, *Phys. Lett. A* **320**, 95 (2003).
- [29] C. Laughlin, B. L. Burrows and M. Cohen, *J. Phys. B* **35**, 701 (2002).
- [30] D. Baye and K. D. Sen, *Phys. Rev. E* **78**, 026701 (2008).
- [31] M. A. Shaqqor and S. M. Al-Jaber, *Int. J. Theor. Phys.* **48**, 2462 (2009).
- [32] H. Ciftci, R. L. Hall and N. Saad, *Int. J. Quant. Chem.* **109**, 931 (2009).
- [33] N. Aquino, G. Campoy and H. E. Montgomery Jr. , *Int. J. Quant. Chem.* **107**, 1548 (2007).
- [34] B. L. Burrows and M. Cohen, *Int. J. Quant. Chem.* **106**, 478 (2006).
- [35] S. Goldman and C. Joslin, *J. Phys. Chem.* **96**, 6021 (1992).
- [36] E. Ley-Koo and S. Rubinstein, *J. Chem. Phys.* **71**, 351 (1979).
- [37] P. W. Fowler, *Mol. Phys.* **53**, 865 (1984).
- [38] H. E. Montgomery Jr. and K. D. Sen, *Int. J. Quant. Chem.* **109**, 688 (2009).
- [39] R. Dutt, A. Mukherjee and Y. P. Varshni, *Phys. Lett. A* **280**, 318 (2001).
- [40] S. H. Patil, *J. Phys. B* **35**, 255 (2002).
- [41] K. D. Sen, J. Garza, R. Vargas and N. Aquino, *Phys. Lett. A* **295**, 299 (2002).
- [42] H. E. Montgomery, *Chem. Phys. Lett.* **352**, 529 (2002).
- [43] C. Laughlin, *J. Phys. B* **37**, 4085 (2004).

- [44] B. L. Burrows and M. Cohen, Phys. Rev. A **72**, 032508 (2005).
- [45] S. Cohen, S. I. Themelis and K. D. Sen, Int. J. Quant. Chem. **108**, 351 (2008).
- [46] B. Çakir, Y. Yakar and A. Özmen, Optics Comm. **311**, 222 (2013).
- [47] J. Gorecki and W. B. Brown, J. Phys. B **20**, 5953 (1987).
- [48] J. L. Marin and S. A. Cruz, J. Phys. B **25**, 4365 (1992).
- [49] K. D. Sen, J. Chem. Phys. **123**, 074110 (2005).
- [50] N. Aquino, A. Flores-Riveros and J. F. Rivas-Silva, Phys. Lett. A **377**, 2062 (2013).
- [51] Y. P. Varshni, Z. Naturforsch A **57**, 915 (2002).
- [52] Y. P. Varshni, J. Phys. B **31**, 2849 (1998).
- [53] K. D. Sen, V. I. Pupyshev and H. E. Montgomery Jr. Adv. Quant. Chem. **57**, 25 (2009).
- [54] N. A. Aquino, Adv. Quant. Chem. **57**, 123 (2009).
- [55] N. A. Aquino and A. Flores-Riveros, in *Electronic Structure of Quantum Confined Atoms and Molecules*, K. D. Sen (Ed.), Springer, pp. 59 (2014).
- [56] A. K. Roy, J. Phys. G **30**, 269 (2004).
- [57] A. K. Roy, Phys. Lett. A **321**, 231 (2004).
- [58] A. K. Roy, J. Phys. B **37**, 4369 (2004), *ibid.* **38**, 1591 (2005).
- [59] A. K. Roy, Int. J. Quant. Chem. **104**, 861 (2005), *ibid.* **113**, 1503 (2013), *ibid.* **114** 383 (2014).
- [60] A. K. Roy, Pramana-J. Phys. **65**, 01 (2005).
- [61] K. D. Sen and A. K. Roy, Phys. Lett. A **357**, 112 (2006).
- [62] A. K. Roy, A. F. Jalbout and E. I. Proynov, Int. J. Quant. Chem. **108**, 827 (2008).
- [63] A. K. Roy, Mod. Phys. Lett. A **29**, 1450042 (2014), *ibid.* **29**, 1450104 (2014).
- [64] J. A. Olson and D. A. Micha, J. Chem. Phys. **68**, 4352 (1978).
- [65] B. Durand and L. Durand, Phys. Rev. D **23**, 1092 (1981).
- [66] J. Lindhard and P. G. Hansen, Phys. Rev. Lett. **57**, 965 (1986).
- [67] A. Bechler and W. Bühring, J. Phys. B **21**, 817 (1988).
- [68] I. S. Bitensky, V. Kh. Ferleger and L. A. Wojciechowski, Nucl. Instrum. Methods Phys. Res. B **125**, 201 (1997).
- [69] R. B. Dingle, Proc. Camb. Phil. Soc. **49**, 103 (1953).
- [70] A. Sinha, R. Roychoudhury and Y. P. Varshni, Can. J. Phys. **78**, 141 (2000).
- [71] Y. P. Varshni, Mod. Phys. Lett. A **19**, 2757 (2004).
- [72] T. Xu, Z.-Q. Cao, Y.-C. Ou, Q.-S. Shen and G.-L. Zhu, Chin. Phys. **15**, 1172 (2006).

- [73] M. Alberg and L. Wilets, *Phys. Lett. A* **286**, 7 (2001).
- [74] R. L. Hall, N. Saad and K. D. Sen, *J. Phys. A* **44**, 185307 (2011).
- [75] F. R. Silva and E. D. Filho, *Chem. Phys. Lett.* **498**, 198 (2010).
- [76] F. R. Silva and E. D. Filho, *Mod. Phys. Lett. A* **25**, 641 (2010).
- [77] M. A. Núñez, *Phys. Rev. A* **47**, 3620 (1993).
- [78] C. Stubbins, *Phys. Rev. A* **48**, 220 (1993).
- [79] B. Gönül, O. Özer, Y. Cangelic and M. Koçak, *Phys. Lett. A* **275**, 238 (2000).
- [80] J. G. Kirkwood, *Phys. Z.* **33**, 57 (1932).
- [81] R. A. Buckingham, *Proc. Roy. Soc. London, Ser. A* **160**, 94 (1937).